Received: 12 February 2024 | Accepted: 4 June 2024

DOI: 10.1111/imm.13825

ORIGINAL ARTICLE

immunology
Insights into immunity in health and disease

CD5L is upregulated upon infection with *Mycobacterium tuberculosis* with no effect on disease progression

Marcos S. Cardoso[1,2] | **Rute Gonçalves**[1,2,3] | **Liliana Oliveira**[1,4] | **Diogo Silvério**[1,3] | **Érica Téllez**[5] | **Tony Paul**[5] | **Maria Rosa Sarrias**[5] | **Alexandre M. Carmo**[1,4] | **Margarida Saraiva**[1,4]

[1]i3S—Instituto de Investigação e Inovação em Saúde, Universidade do Porto, Porto, Portugal

[2]ESS, Politécnico do Porto, Porto, Portugal

[3]Doctoral Program in Molecular and Cell Biology, ICBAS-Instituto de Ciências Biomédicas Abel Salazar, Universidade do Porto, Porto, Portugal

[4]IBMC—Instituto de Biologia Molecular e Celular, Universidade do Porto, Porto, Portugal

[5]Innate Immunity Group, Germans Trias i Pujol Research Institute (IGTP), Badalona, Spain

Correspondence
Margarida Saraiva, i3S, Rua Alfredo Allen 208, 4200-135 Porto, Portugal.
Email: margarida.saraiva@i3s.up.pt

Funding information
Fundação para a Ciência e a Tecnologia, Grant/Award Numbers: CEECIND/00241/2017, PTDC/SAU-INF/1172/2021, 2022.12852.BD, SFRH/BD/143536/2019; 'la Caixa' Foundation, Grant/Award Number: HR21-00415; EU's Horizon 2020 Research and Development Program, Grant/Award Number: nº 847762; Catalan Agency for Management of University and Research, Grant/Award Number: 2021-SGR-01186

Abstract

Tuberculosis (TB) alone caused over a billion deaths in the last 200 years, making it one of the deadliest diseases to humankind. Understanding the immune mechanisms underlying protection or pathology in TB is key to uncover the much needed innovative approaches to tackle TB. The scavenger receptor cysteine-rich molecule CD5 antigen-like (CD5L) has been associated with TB, but whether and how CD5L shapes the immune response during the course of disease remains poorly understood. Here, we show an upregulation of CD5L in circulation and at the site of infection in C57BL/6 *Mycobacterium tuberculosis*-infected mice. To investigate the role of CD5L in TB, we studied the progression of *M. tuberculosis* aerosol infection in a recently described genetically engineered mouse model lacking CD5L. Despite the increase of CD5L during infection of wild-type mice, absence of CD5L did not impact bacterial burden, histopathology or survival of infected mice. Absence of CD5L associated with a modest increase in the numbers of CD4+ T cells and the expression of IFN-γ in the lungs of infected mice, with no major effect in overall immune cell dynamics. Collectively, this study confirms CD5L as a potential diagnostic biomarker to TB, showing no discernible impact on the outcome of the infection.

KEYWORDS
CD5L, immune response, macrophage, T cells, tuberculosis

INTRODUCTION

In 2022 alone, more than 10 million individuals fell ill with tuberculosis (TB) and 1.3 million died of the disease [1]. Elucidating the immune mechanisms of TB

Marcos S. Cardoso, Rute Gonçalves, Alexandre M. Carmo and Margarida Saraiva contributed equally to this study.

pathogenesis can offer insights on candidate molecules to be used from a diagnostic or prognostic point of view, and potentially be further developed into novel prophylactic or therapeutic candidates.

Several molecules are altered in the blood, urine or saliva of TB patients [2], among which the scavenger receptor cysteine-rich protein CD5 antigen-like (CD5L) [3–5]. CD5L, a secreted glycoprotein mainly produced by tissue-resident macrophages [6, 7], plays distinct roles, from functioning as an anti-apoptotic protein [8] to a role as a pattern recognition receptor (PRR) [9, 10], participation in autophagy [11], regulation of lipid metabolism [12], among others [13]. This multifunctionality directly impacts the modulation of several key immunological events, including infection [13]. CD5L is upregulated in the serum of both humans and mice upon *Mycobacterium tuberculosis* infection [3–5], and improves the microbicidal capacity of human macrophages infected with *M. tuberculosis* in vitro [4]. More recently, CD5L was also found to be upregulated in high-burden granulomas of *M. tuberculosis*–infected rhesus macaques in comparison with low-burden granulomas. Interestingly, the gene signature of high-burden granulomas exhibited markers associated with type 2 immune responses, possibly linking CD5L to wound-healing responses [14].

Collectively, these observations suggest a putative role for CD5L during *M. tuberculosis* infection. However, whether and how the upregulation of CD5L influences the outcome of TB remains to be elucidated. Here, we show that CD5L expression was highly induced not only in the blood, but also in lungs of *M. tuberculosis*-infected mice. Although the abrogation of this molecule did not significantly impact TB susceptibility or progression, the absence of CD5L associated with an increase in lung CD4+ T cells and interferon (IFN)-γ production upon *M. tuberculosis* infection in vivo. In vitro, CD5L deficiency did not impact the overall response of resident or bone marrow-derived mouse macrophages to *M. tuberculosis* infections. Thus, our study reinforces the potential of CD5L as a TB biomarker, while calling for further investigation to establish a possible bridge between CD5L expression and T cell function.

MATERIALS AND METHODS

Ethics approval

Animal experiments performed at the i3S Animal Facility were approved by the i3S Animal Ethics Committee and Portuguese Competent Authority (DGAV) in accordance with the European Union Directive 2010/63/EU and Portuguese Legislation. The i3S animal facility is AAALAC accredited.

Bacteria growth

M. tuberculosis HN878 isolate was grown in Middlebrook 7H9 liquid medium (BD Biosciences, 271 310) supplemented with 10% OADC and 0.2% glycerol at 37°C with agitation. At mid-log phase, bacterial suspensions were frozen and stored at −80°C. Viable bacteria were determined by colony forming unit (CFU) enumeration of serial dilutions of bacteria in 7H11 (BD Biosciences, 212 203) agar plates, after incubation at 37°C for 21–28 days.

Animal housing and aerosol infection

CD5L deficient (KO) mice were generated using the CRISPR/Cas9 system, as described [15]. All the details, including the validation of the model with regard to abrogation of CD5L protein, are shown in the original manuscript [15]. C57BL/6 wild-type (WT) or CD5L-KO mice were bred and housed at the i3S Animal House Facility. Both male and female mice, with 8–12 weeks of age, were aerosol infected with *M. tuberculosis* HN878 in the ABSL3 lab. Mice were kept under a controlled temperature (20–24°C), humidity (45–65%) and light cycle (12 h light/dark) in specific-pathogen free conditions. Water and food were provided ad libitum. Infection was performed using the Glas-Col inhalation exposure system, as described [16]. Dose of infection was determined based on lung CFU at day 3 post-infection. Doses below 200 CFU were considered low, whereas above 500 CFU were considered high doses. Infected mice were weighed every week, or every other day when showing signs of disease. Mice were euthanised at the indicated timepoints or when reaching humane endpoints (weight loss over 20% or poor responsiveness to physical stimulation).

Organ processing

Infected mice were euthanised by CO_2 inhalation. Blood was collected via cardiac puncture and serum separated by centrifugation. Lungs were aseptically excised after cardiac perfusion with PBS and digested using Collagenase type IV (Gibco, 17 104 019) followed by physical disruption and filtering in a 70 μm strainer. The right upper lung lobe was used to histological analysis. Single-cell suspensions were used for bacterial burden determination, flow cytometry and RNA analysis. Bacterial CFU in infected lungs were performed as above.

Histological analysis

Mouse lung lobes were fixed in 10% buffered neutral formalin and embedded in paraffin. Four-µm sections were used for haematoxylin and eosin (H&E) staining or immunohistochemistry (IHC). Morphometric analysis of lung pathology of H&E-stained histological sections was performed using the software Interactive Learning and Segmentation Toolkit (Ilastik version 1.3.3) and CellProfiler Analyst (version 3.1.5), as before [17]. Number of lesions per section was calculated using the same software and non-infected (NI) lungs as baseline. H&E images were acquired with a NanoZoomer 2.0-HT Whole Slide Imager, Digital Pathology Slide Scanner.

Immunohistochemistry

IHC staining was performed by standard protocol: deparaffinised with xylene, followed by rehydration in graded alcohol concentration. Endogenous peroxidase blocking was performed with 0.3% H_2O_2 in ethanol during rehydration. Heat-induced antigen retrieval (HIER) was performed in Citrate buffer (pH 6, 10×, Sigma–Aldrich, C-9999) at 121°C for 10 min, followed by permeabilisation with 0.2% Tween in PBS for 10 min. Slides were later incubated with anti-CD5L (R&D Systems, AF2834) dissolved in blocking buffer (3% BSA (Sigma–Aldrich, A4503-504) +5% donkey serum [Millipore, Merck, S30 and S26, respectively]), overnight at 4°C. Donkey anti-goat IgG-HRP (Jackson ImmunoResearch, AB_2340390, RRID: AB_2340390) was used as secondary antibody for 30 min. Chromogenic detection of antibody binding was performed using a Liquid-DAB substrate (Agilent Technologies, K346711-2). Counterstaining was done with haematoxylin (Merck, 1 051 740 500, HX 86017674). Slides were later mounted with DPX (Sigma–Aldrich, DPX 06522), dried, and observed under a Leica DMI6000B microscope (Leica Microsystems). For quantification, captured images were analysed using Image J, colour deconvolution 2 plugin.

RNA extraction and RT-qPCR

RNA extraction from tissue was performed using the RNeasy Mini Kit (Qiagen, 74 106) or the TRIzol reagent (GRiSP, GB23.0100), following manufacturer's instructions. Total RNA (1 µg) was reverse transcribed to cDNA using EcoDry™ Premix (Clontech, 639 549) or ProtoScript cDNA synthesis kit (New England BioLabs, E6300S). For *Cd5l* gene expression, each RT reaction was then amplified in a LightCycler® 480 PCR system using the TB Green Premix EX Taq (Takara, RR42WR). mRNA expression of *Tnfa*, *Il6*, *Ifnb*, *Ifng* and *Il17* were quantified using a CFX Connect™ Real-Time PCR Detection System (Bio-Rad) and a SYBR green dye (Biorad, 1 708 880). Oligonucleotides used are listed in Table S1. Gene expression values were normalised to the expression levels of *18 s* (18 s ribosomal RNA) or *Ubiquitin* and *Gapdh* for *Cd5l* or *Tnfa*, *Il6*, *Ifnb*, *Ifng* and *Il17*, respectively. Fold induction levels were calculated using the average level of expression of each gene in control samples as reference.

Flow cytometry analysis

Mouse lung cell suspensions were stained for surface antigens for 30 min and fixed for 20 min in 4% paraformaldehyde-PBS. Dead cells were excluded from the analyses using Zombie Green (Biolegend, 423 112) viability dye. Cells were acquired on a BD FACS Canto II (BD Biosciences). Data were analysed using FlowJo (version 10.1.r7). Antibodies used are listed in Table S2.

Bone marrow-derived macrophage culture

The bone marrow was collected from NI WT and CD5L-KO mice by flushing the tibias and femurs with PBS + 2% foetal bovine serum (FBS) (Gibco, 10 500 064). BMDM (bone marrow-derived macrophage) were differentiated from bone marrow precursors using 20% L929 cell-conditioned media (LCCM). On day 7, cells were harvested and cultured in 24-well tissue plates at a concentration of 0.5×10^6 cells/well in complete medium (cDMEM): Dulbecco's Modified Eagle Medium (DMEM) (Gibco, 10 566 016) supplemented with 10% FBS (Gibco, 10 500 064), 1% HEPES (Gibco, 15 630 106).

Alveolar macrophage culture

For alveolar macrophage (AM) collection, NI WT and CD5L-KO mice were euthanised by intraperitoneal injection of sodium pentobarbital (400 mg/kg). The bronchoalveolar lavage was recovered through canulation of the trachea and collection of liquid in sterile PBS +1% FBS. Cells were centrifuged, counted and seeded in 96-well tissue plates at a concentration of 5×10^4 cells/well in Roswell Park Memorial Institute (RPMI) (Gibco, 61 870 044) supplemented with 10% FBS.

In vitro infections

After overnight resting, BMDM and AM were infected with *M. tuberculosis* HN878 at a multiplicity of infection

(MOI) of 2. Uninfected cells were used as negative controls. At 4 h and 4 days post-infection, cells were lysed with 0.1% saponin (Sigma, S-7900) and CFU were enumerated as above. Culture supernatants were recovered 24 h post-infection, filter-sterilised and used for cytokine quantification.

Cytokine quantification

Mouse CD5L serum levels and cell supernatant cytokine quantification of TNF-α, IL-10 and IL-6 (Thermo Fisher Scientific EM15RB, 88-7324-88, 88-7105-88 and 88-7064-88, respectively) were measured by enzyme linked immunosorbent assay (ELISA) following manufacturer's instructions.

Statistical analysis

Data were analysed using GraphPad Prism software v8.1.0 or R v4.1. Every dataset was tested for outliers, statistical normality and homogeneity of variances, and based on this information, an appropriate statistical test was used. Statistically significant differences between two groups were determined using unpaired *t* test or Mann–Whitney *U* tests. One Way ANOVA test was used to determine multiple comparisons between more than two groups. Differences were considered significant for $p \leq 0.05$ and represented as follows: $^{*}p \leq 0.05$; $^{**}p \leq 0.01$; $^{***}p \leq 0.001$ and **** $p \leq 0.0001$.

RESULTS

CD5L expression is upregulated upon *M. tuberculosis* infection

Levels of circulating CD5L increase dramatically in several immune conditions [18–22], including in mice infected with *M. tuberculosis* [4, 5]. Nevertheless, levels of CD5L in the lungs (site of infection) and the putative role of CD5L during *M. tuberculosis* infection remain uncharacterised. To measure the expression of CD5L at the infection site, we started by interrogating a previously published RNA-seq dataset, in which the lung transcriptional response of TB-resistant (C57BL/6) or TB-susceptible (C3HeB-FeJ) mice infected with low or high doses of *M. tuberculosis* laboratory strain H37Rv or the hypervirulent isolate HN878 were analysed at the peak of disease [23]. Independently of the mouse and bacteria genetic backgrounds, we found a clear upregulation of *Cd5l* in the lung upon *M. tuberculosis* infection (Figure 1a,b). Although the expression of *Cd5l* was upregulated in *M. tuberculosis*-infected C57BL/6 mice as compared to non-infected controls, no discernible differences were detected among the infected mice, irrespective of the strain and dose of bacteria used (Figure 1a). However, in C3HeB-FeJ mice, we found a higher *Cd5l* gene expression in *M. tuberculosis* HN878 infections as compared to those with H37Rv (Figure 1b). Using matching datasets, we analysed the expression of *Cd5l* in the blood of C57BL/6 and C3HeB-FeJ mice. Although no major differences were found between NI and *M. tuberculosis*-infected C57BL/6 mice, we observed a significant upregulation of *Cd5l* in the blood of all *M. tuberculosis*-infected C3HeB-FeJ mice, compared with C3HeB/FeJ NI mice (Figure S1a,b).

To validate the *Cd5l* expression profile obtained through the interrogation of the RNA-Seq datasets, C57BL/6 mice were aerosol-infected with high doses of *M. tuberculosis* HN878. On day 30 post-infection, lung samples were analysed by PCR or IHC to assess *Cd5l* mRNA and protein levels, respectively. We found a significant upregulation of CD5L levels at the site of infection both at mRNA (Figure 1c) and protein (Figure 1d) levels, in *M. tuberculosis*-infected mice. Lung CFU numbers were also assessed to control for disease progression (Figure S1c). In addition, we measured circulating levels of CD5L in the serum and, as anticipated [4], observed an increase of CD5L in *M. tuberculosis*-infected mice, compared to NI mice (Figure 1e). We next aerosol-infected WT mice with low doses of *M. tuberculosis* HN878, or IFN-γ-KO mice with high doses of this isolate. As expected, the bacterial burdens obtained on day 30 post-infection for the low dose infections were lower than those obtained for the high dose ones, whereas IFN-γ-KO mice presented higher bacterial burdens (Figure S1d). Compared to NI mice, the increase in circulating CD5L levels were higher in C57BL/6 mice infected with high than with low doses of *M. tuberculosis* HN878 (∼27-fold vs. ∼12-fold; Figure 1f). Moreover, the highly susceptible IFN-γ-KO mice displayed an even higher amount of circulating CD5L (∼32-fold increase, compared with NI; Figure 1f). These findings suggest that increased CD5L circulating levels may reflect increased bacterial burdens in the mouse experimental models studied herein.

CD5L abrogation does not impact the outcome of in vivo *M. tuberculosis* infections

To assess the functionality of CD5L during *M. tuberculosis* in vivo infection, we compared the dynamics of disease

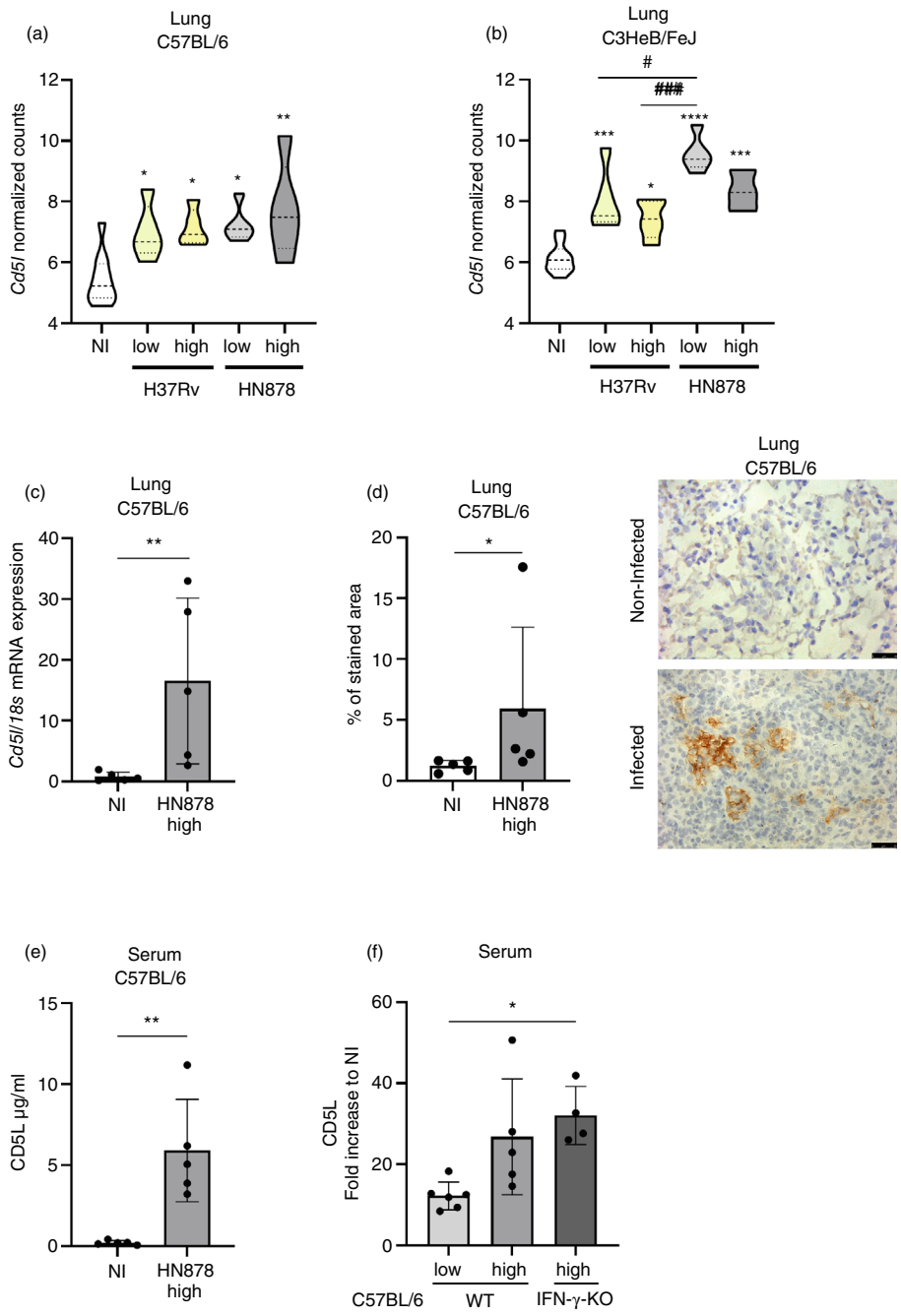

FIGURE 1 Increased expression of CD5L in *Mycobacterium tuberculosis*-infected mice. Expression of *Cd5l* in the lungs of TB-resistant C57BL/6 (a) or TB-susceptible C3HeB/FeJ (b) animals aerosol-infected with low or high doses of *M. tuberculosis* H37Rv or HN878, as indicated. Non-infected (NI) animals are shown as controls. Data are normalised counts obtained from RNA-Seq datasets from [23]. Statistical analysis was performed using one-way ANOVA test to multiple comparisons between groups. Statistical differences in comparison to NI animals are indicated with *. C57BL/6 mice were left NI or were aerosol infected with high doses of *M. tuberculosis* HN878. Thirty days post infection (p.i.) the lungs were harvested and used for quantification of (c) *Cd5l* mRNA normalised to *18 s*; and (d) CD5L by immunohistochemical analysis. Percentage of CD5L stained area (left panel) and representative images of NI and infected lungs (right panel) are shown. Scale bars: 25 µm. At the same time-point, the serum was harvested and (e) CD5L levels detected by ELISA. (f) Fold increase of CD5L levels in the serum of C57BL/6 wild-type (WT) infected with different bacterial doses and IFN-γ-knockout (KO) compared to NI animals. (c–f) Represented is the Mean ± SD for each experimental group. Each dot represents one animal. The bacterial doses delivered to the lung and measured at the end-point for each infection are shown in Figure S1c,d. Statistically significant differences between two groups were determined using Mann–Whitney *U* tests and comparisons between more than two groups were determined using one-way ANOVA. Differences between groups were considered significant if $p < 0.05$; *$p \leq 0.05$; **$p \leq 0.01$; ***$p \leq 0.001$ and ****$p \leq 0.0001$.

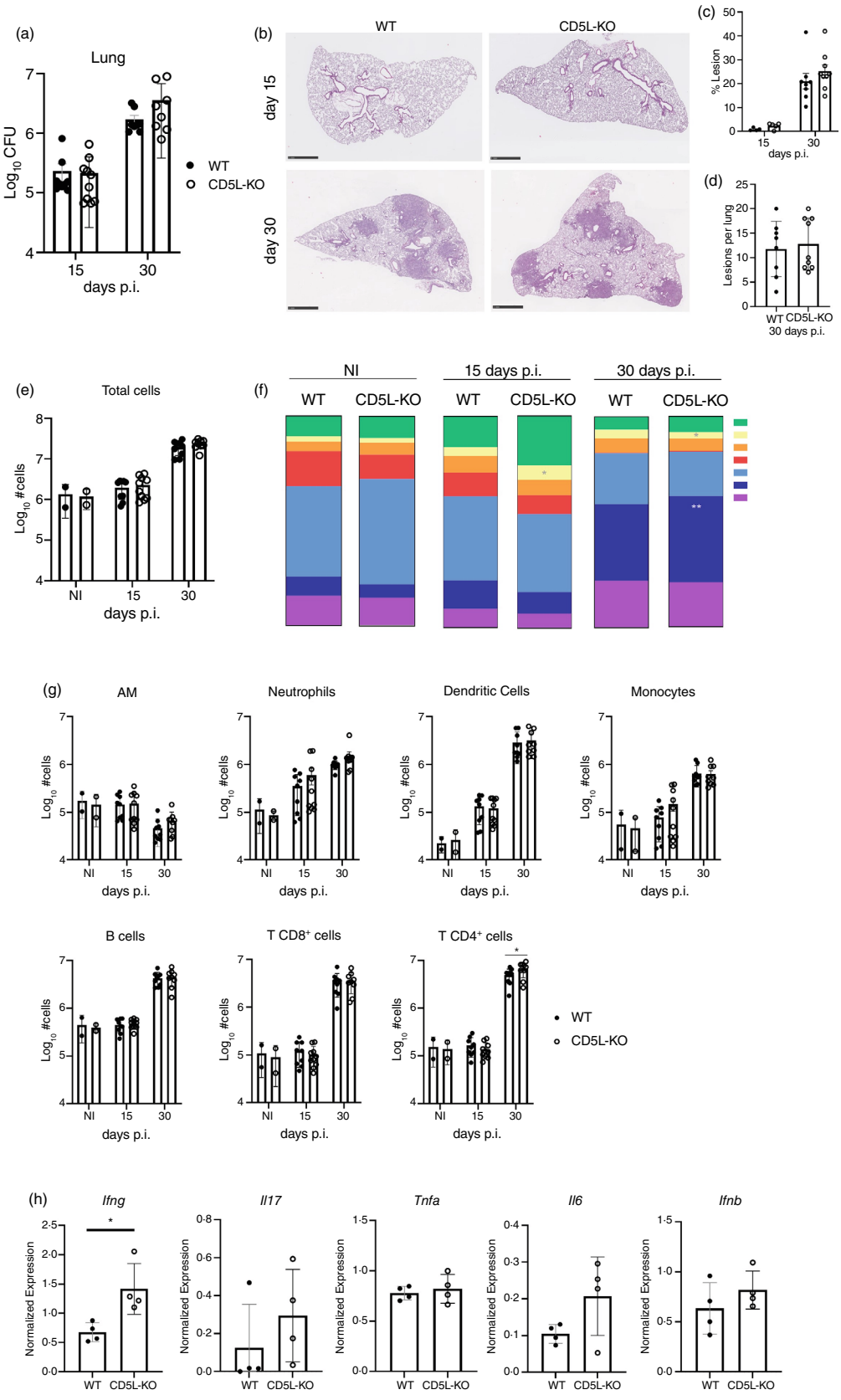

FIGURE 2 Role of CD5L in early resistance/susceptibility to *Mycobacterium tuberculosis* infection. C57BL/6 wild-type (WT; closed circles) and CD5L-knockout (KO; open circles) mice were aerosol-infected with low doses of *M. tuberculosis* HN878. Two independent experiments were performed. (a) Bacterial burden in the lungs on days 15 and 30 post-infection (p.i.). (b) Representative images of haematoxylin and eosin (H&E) lung sections for the indicated mice strains and times of infection. Scale bars: 1 mm. (c) Percentage of area of lesion (% lesion) and (d) number of lesions per lung quantified in lung sections of mice infected for 30 days. (e) Total number of lung cells in infected WT and CD5L-KO animals on days 15 and 30 p.i. Frequency (f) and total cell counts (g) of distinct myeloid and lymphoid cell populations in non-infected (NI) and *M. tuberculosis*-infected mice on days 15 and 30 p.i. Gating strategy is shown in Figure S2e. (h) Relative expression of the indicated cytokine genes in the lung of infected WT and CD5L-KO animals 30 days p.i. Expression was normalised using *Gapdh* and *Ubiquitin* reference genes. Data are Mean ± SD and each dot represents an individual mouse. The statistical analyses were performed using unpaired *t* test or Mann–Whitney *U* test to identify statistical differences between groups. Differences between groups were considered significant if $p < 0.05$ and represented as follows: $*p \leq 0.05$.

progression in C57BL/6 WT and CD5L-KO mice upon aerosol-infection with low doses of the hypervirulent *M. tuberculosis* HN878 isolate. No significant differences in lung bacterial loads were observed between WT and CD5L-KO mice at days 15 or 30 post-infection (Figure 2a). Similarly, no differences were observed in weight loss

between the two experimental groups over the course of the experiment (Figure S2a). Furthermore, CD5L abrogation did not impact pulmonary histopathology (Figure 2b), specifically the percentage of infiltrated area (Figure 2c) or the number of lesions (Figure 2d) per lung lobe. Of note, the number of lesions were only quantified on day 30 as they were basically inexistent on day 15 post-infection (Figure 2b).

Next, we questioned whether CD5L deficiency might impact the susceptibility to infection of C57BL/6 mice with a higher dose of *M. tuberculosis* HN878 isolate. This model is characterised by neutrophil-mediated inflammation, severe lung damage and increased susceptibility [24, 25]. No differences were observed in susceptibility to *M. tuberculosis* infection between WT (50% survived) and CD5L-KO mice (58.3% survived) during the experimental duration (Figure S2b). Also, no differences were observed in weight variation of the infected mice (Figure S2c). On day 47 post-infection, surviving mice were sacrificed and their lung bacterial counts determined, with no differences observed between WT and CD5L-KO mice (Figure S2d). Collectively, data obtained from experimental *M. tuberculosis* HN878 infection with two different doses suggest that CD5L deficiency does not impact survival, bacterial burden or histopathology features of infection.

CD4+ T cell recruitment and IFN-γ production are enhanced in the absence of CD5L

CD5L modulates immune cell recruitment either by acting directly, as a chemoattractant, or indirectly, by inducing/modulating the expression of chemokines [21, 26]. Thus, we questioned whether CD5L would modulate immune cell recruitment to the lungs of *M. tuberculosis* infected mice. No differences were found between the numbers of live cells in WT and CD5L-KO lungs on days 15 and 30 post-infection (Figure 2e). We next analysed by flow cytometry the dynamics of the lung immune compartment at days 15 and 30 post-infection. Importantly, during steady-state conditions no differences were observed in the lung immune cell compartment of WT or CD5L-KO mice (Figure 2f; gating strategy in Figure S2e). Infection with *M. tuberculosis* HN878 isolate led to a rapid recruitment of neutrophils followed by a persistent influx of T cells in WT mice (Figure 2f). Although not significant, the frequency of neutrophils in the lungs of CD5L-KO mice at day 15 post-infection was slightly higher than that observed in WT mice (Figure 2f). The frequency of monocytes was statistically increased in CD5L-KO mice after 15-days post-infection, but reduced after 30-days post-infection, whereas that of CD4+ T cells was statistically higher in CD5L-KO mice 30-days post-infection (Figure 2f). However, statistically significant differences were only observed for CD4+ T cell numbers, which were higher in infected CD5L-KO mice (Figure 2g). All other innate (AM, neutrophils, dendritic cells, monocytes) and acquired (B cells or CD8+ T cells) immune cell populations were identical in the two mice (Figure 2g). We next assessed the lung expression of several genes at day 30 post *M. tuberculosis* infection by q-PCR. In line with the increased numbers of CD4+ T cells, expression of *Ifng* was augmented in CD5L-KO mice, whereas the expression of the other tested genes was similar between WT and CD5L-KO mice (Figure 2h). The expression of *Il10* was also assessed but not detected.

CD5L deficiency does not impact in vitro macrophage *M. tuberculosis* uptake and control

Although CD5L is a well-established PRR capable of binding to bacteria, its role in enhancing the phagocytosis of live bacteria or bacterial particles remains controversial [27–29]. Interestingly, overexpression of human CD5L in THP-1 cells did not enhance *M. tuberculosis* phagocytosis [4]. We investigated the possible contribution of CD5L in mediating the phagocytosis or killing of *M. tuberculosis* by AM or BMDM. Whereas AM are resident lung macrophages that establish the first contact with *M. tuberculosis*, BMDM represent a model for blood monocytes/macrophages recruited to infected lungs replacing AM as the main niche for *M. tuberculosis* survival at later time points [30, 31]. For this, we infected WT and CD5L-KO AM or BMDM with *M. tuberculosis* HN878 isolate and analysed the bacterial burden 4 h or 4 days post-infection. No differences were found between WT and CD5L-KO cells for the bacterial burden at 4 h post-infection, which suggests identical bacteria internalisation (Figure 3a,b). Similarly, after 4 days of culture, CFU counts indicated that WT and CD5L-KO AM or BMDM had similar killing efficiencies (Figure 3a,b). Overall, these results indicate that CD5L abrogation did not impact phagocytosis or bacteria killing.

Finally, we analysed secretion of TNF-α, IL-6, and IL-10 by WT or CD5L-KO AM or BMDM at 24 h post-infection by immunoassay. No differences in secretion of TNF-α or IL-6 were observed between WT or CD5L-KO AM or BMDM upon infection (Figure 3c). Although IL-10 was undetected in the supernatants of infected AM (Figure 3c), in infected BMDM, a small decrease was observed in the case of CD5L-KO cultures (Figure 3d).

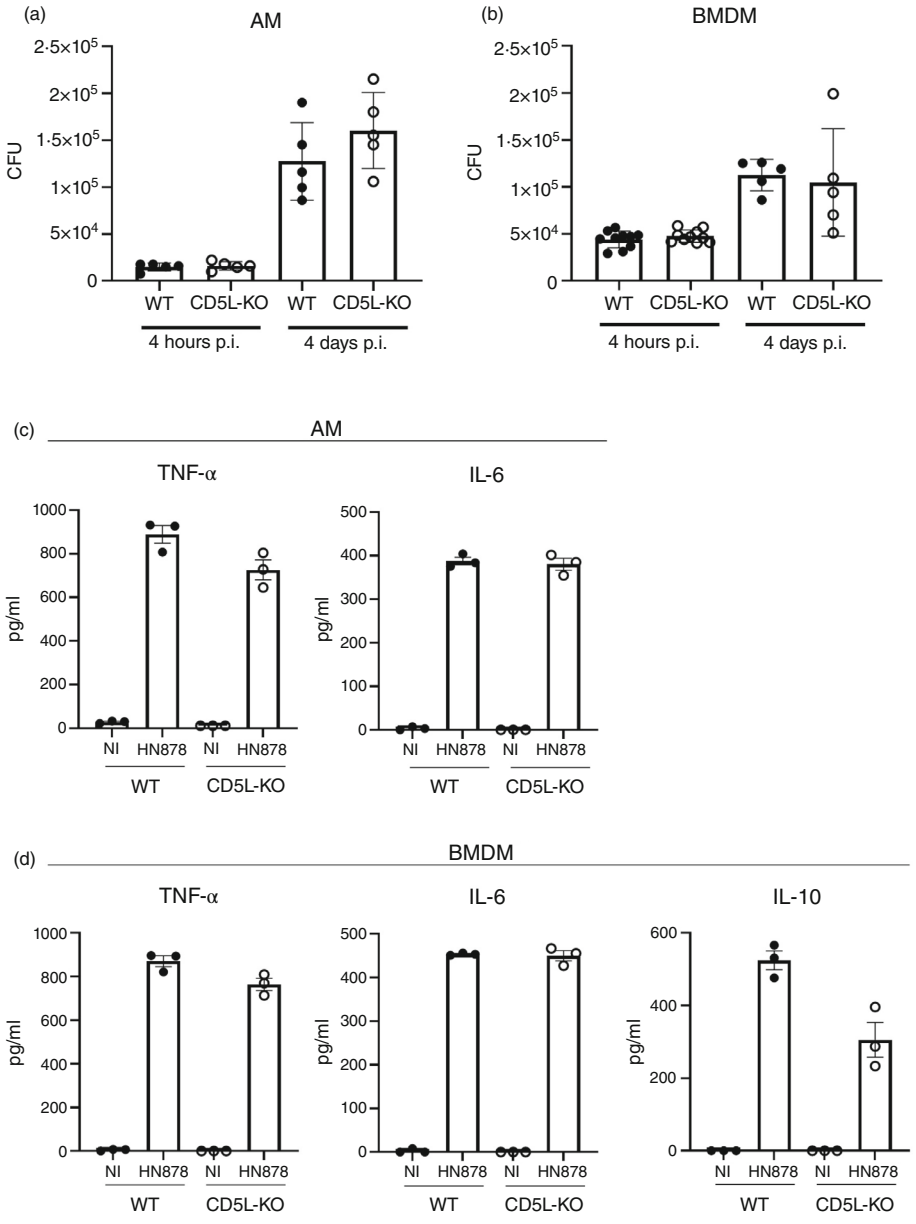

FIGURE 3 Role of CD5L in regulating the macrophage response to *Mycobacterium tuberculosis* infection. Mouse alveolar macrophages (AM) and bone marrow-derived macrophages (BMDM) from wild-type (WT; closed circles) and CD5L-knockout (KO; open circles) mice were cultured and in vitro infected with *M. tuberculosis* HN878 at a multiplicity of infection (MOI) of 2. Bacterial loads of AM (a) and BMDM (b), determined at 4 h and 4 days post infection (p.i.). Cytokines levels of TNF-α, IL-6 and IL-10 measured in the supernatants of non-infected (NI) or *M. tuberculosis* HN878-infected AM (c) or BMDM (d) 24 h p.i. IL-10 was undetected in AM. Data are Mean ± SD. The statistical analyses were performed using Mann–Whitney *U* test to identify statistical differences between groups.

Collectively, these data suggest that the absence of CD5L did not generally impact the response of AM or BMDM to *M. tuberculosis*.

DISCUSSION

Multiple studies consider CD5L as a potential biomarker for a wide range of human diseases, including bacterial infection [18], sepsis [19], type 2 diabetes [20], hepatocellular carcinoma [32], liver fibrosis [21] and systemic lupus erythematosus [22]. Likewise, CD5L has been linked to active TB in humans, as its circulating levels are upregulated in patients with active TB before treatment initiation in comparison with healthy subjects [3]. Complementary data from experimental mouse infections showed a prompt increase in circulating levels of CD5L upon aerosol (C57BL/6) or intravenous (C3HeB/FeJ) infections with the *M. tuberculosis* laboratory strain H37Rv, peaking at 3 weeks post-infection and followed by a subsequent decrease [4, 5]. Our data obtained by interrogating previously published RNA-seq datasets [23] of blood and lung of *M. tuberculosis*-infected C57BL/6 or C3HeB/FeJ mice at the peak of disease confirm these reports. Furthermore, we show that the overwhelming immune response induced by the hypervirulent *M. tuberculosis* HN878 isolate resulted in the strongest upregulation of the levels of CD5L in circulation and also at the site of infection. By measuring CD5L in the serum of different mouse models, our data suggest a potential link between the amount of circulating CD5L and bacterial burdens. Of note, significant differences in RNA

levels of *Cd5l* were not detected using the RNA-seq datasets of C57BL/6 versus C3HeB/FeJ mice, despite their different susceptibility to *M. tuberculosis* infection. This likely reflects differences between transcriptional and protein data. Regardless, our findings support CD5L as a candidate biomarker for TB. Further studies in human cohorts of TB are needed to explore this hypothesis.

We next sought to investigate whether the upregulation of CD5L in *M. tuberculosis* infected lungs might impact the local immune response and TB outcome. We used a recently described CD5L-KO mouse [15] aerosol-infected with *M. tuberculosis* HN878. This hypervirulent *M. tuberculosis* isolate is characterised by enhanced type I IFN, dysregulated Th1 responses, and exacerbated neutrophil recruitment, leading to extensive histopathology [24, 25]. Despite the CD5L upregulation observed at the site of infection, absence of this molecule did not impact bacterial burden, histopathology, or mice survival, suggesting that CD5L is most likely not required for protection during mycobacterial infections. Although lack of CD5L did not impact the outcome of infection even when mice were infected with low doses of *M. tuberculosis* HN878, we cannot discard a potential effect of this molecule in less virulent *M. tuberculosis* infections or at later times post-infection. As the CD5L-KO model used was generated in a C57BL/6 genetic background, we cannot also exclude a role for CD5L in *M. tuberculosis* infections of C3HeB/FeJ mice. Addressing the impact of abrogating CD5L in *M. tuberculosis*- infected C3HeB/FeJ mice might prove interesting as these mice showed higher expression of *cd5l* mRNA than C57BL/6, as detected by RNAseq analysis. As CD5L is mainly produced by tissue macrophages and these are important target cells for *M. tuberculosis*, one could speculate that this interaction triggers CD5L release. However, the intracellular nature of the pathogen keeps it protected from, at least, the CD5L opsonisation-like effect, which might explain the lack of impact of CD5L absence.

CD5L is a pleiotropic molecule that exerts a wide range of functions, including T-cell modulation [12, 33, 34]. Previous studies have reported that loss of CD5L converts non-pathogenic Th17 cells into pathogenic Th17 ones [12]. Additionally, a role for CD5L in CD4+ T cell differentiation was proposed through modulation of the IL-6/IL-12 cytokine family. Specifically, CD5L may associate with p19 [34] and p40 subunits [34, 35] to form p19/CD5L and p40/CD5L heterodimers. Thus, CD5L may play a role in IL-12 (p35/p40) and IL-23 (p19/p40) modulation, critical for Th1 and Th17 cell differentiation [36, 37]. Furthermore, although the function of p40/CD5L remains poorly understood, the heterodimer p19/CD5L impacts directly in T cell proliferation, STAT5 phosphorylation, and increase of granulocyte macrophage colony-stimulating factor (GM-CSF)-producing CD4+ T cells [34]. Interestingly, during *M. tuberculosis* infection, abrogation of CD5L led to an increase of CD4+ T cells that is further accompanied by augmented expression of *Ifng*, potentially disclosing a novel role for CD5L in modulating lung T cell responses. Moreover, we observed a slight but not statistical increase in the percentage of infiltrated area and total immune cells in the lungs of CD5L-KO mice, suggesting a greater influx of immune cells in the absence of CD5L. Overall, these findings indicate that the absence of CD5L during *M. tuberculosis* infection may contribute to an amplified pro-inflammatory Th1 response. Further studies are needed to elucidate a possible role for the CD5L protein in Th1 cell differentiation in the context of *M. tuberculosis* infections and whether this may be linked to p40/p19-CD5L heterodimers. Another possible explanation for the increase of Th1 cells in the absence of CD5L may be linked to the impact of this molecule on IL-10. Our data suggest a decrease of IL-10 production by *M. tuberculosis*-infected in the absence of CD5L. Because IL-10 is a known negative regulator of Th1 cell differentiation via acting on antigen presenting cells [38], our in vitro and in vivo observations may be linked. However, as we did not detect *Il10* expression in whole lungs, this hypothesis awaits further investigation.

We here show that phagocytosis of *M. tuberculosis* by AM or BMDM was not influenced by the absence of CD5L. This is in accordance with a previous study demonstrating that *M. tuberculosis* phagocytosis was not enhanced in THP-1 cells overexpressing the human form of CD5L [4]. However, while overexpression of CD5L in THP-1 cells resulted in improved mycobactericidal responses [4], we show that its absence did not affect the ability of AM or BMDM to control *M. tuberculosis* over time. This apparent discrepancy may reflect differences between human and mouse macrophages, cell lines and primary cells, or may highlight a dose–response effect of CD5L (as in the case of THP-1 cells overexpression, not deletion, of CD5L was tested) suggesting a therapeutic potential for CD5L overexpression in *M. tuberculosis* infections. Investigating this hypothesis will require an experimental setup where recombinant CD5L is administered in vivo, rather than abrogated, during infection.

In summary, our study reinforces the upregulation of CD5L upon *M. tuberculosis* infections, adding value to the potential of CD5L as a biomarker. However, increase in the expression of CD5L in the lung and serum of infected mice does not translate into altered protection or susceptibility to *M. tuberculosis* infection. Finally, our findings also highlight a possible role for CD5L in regulating T cell responses in TB.

AUTHOR CONTRIBUTIONS

Investigation: MSC, RG, LO, DS, ET, TP. *Project administration*: MRS, AMC, MS. *Resources*: AMC. *Supervision*: MRS, AMC, MS. *Validation*: MSC, RG, MRS, MS. *Visualisation*: MSC, RG, ET. Writing—original draft: MSC, RG, MRS, AMC, MS. Writing—review and editing: all authors.

ACKNOWLEDGEMENTS

We acknowledge the i3S scientific platforms Translational Cytometry and Animal House. We also acknowledge Dr. Cristina Vilaplana for critical review of the manuscript.

FUNDING INFORMATION

This work has been funded by La Caixa Foundation (HR21-00415) and the Portuguese Foundation for Science and Technology (FCT; grant PTDC/SAU-INF/1172/2021) to MS. RG and DS hold FCT PhD fellowships with references 2022.12852.BD and SFRH/BD/143536/2019, respectively. TP holds a fellowship from ISCIII, Spanish Government: PFIS (FI20/00115). This study received funding from the EU's Horizon 2020 Research and Development Program under grant agreement n° 847 762. The Innate Immunity lab is accredited by the Catalan Agency for Management of University and Research Grant 2021-SGR-01186. MRS is a researcher at IGTP, which is a member of the CERCA network of institutes supported by the Health Department of the Government of Catalonia. MS is funded by FCT through CEECIND/00241/2017.

CONFLICT OF INTEREST STATEMENT

A patent protecting a method for the detection of CD5L has been submitted to the European Patent Office (EP3653646A1) (MRS).

DATA AVAILABILITY STATEMENT

The data that support the findings of this study are available from the corresponding author upon reasonable request.

ORCID

Marcos S. Cardoso https://orcid.org/0000-0003-0150-7359
Diogo Silvério https://orcid.org/0000-0003-2254-1230
Margarida Saraiva https://orcid.org/0000-0002-8180-1293

REFERENCES

1. Organization WH. Global tuberculosis report 2023. 2023.
2. MacLean E, Broger T, Yerlikaya S, Fernandez-Carballo BL, Pai M, Denkinger CM. A systematic review of biomarkers to detect active tuberculosis. Nat Microbiol. 2019;4(5):748–58.
3. Xu DD, Deng DF, Li X, Wei LL, Li YY, Yang XY, et al. Discovery and identification of serum potential biomarkers for pulmonary tuberculosis using iTRAQ-coupled two-dimensional LC-MS/MS. Proteomics. 2014;14(2–3):322–31.
4. Sanjurjo L, Amézaga N, Vilaplana C, Cáceres N, Marzo E, Valeri M, et al. The scavenger protein apoptosis inhibitor of macrophages (AIM) potentiates the antimicrobial response against *Mycobacterium tuberculosis* by enhancing autophagy. PLoS One. 2013;8(11):e79670.
5. Kroesen VM, Rodríguez-Martínez P, García E, Rosales Y, Díaz J, Martín-Céspedes M, et al. A beneficial effect of low-dose aspirin in a murine model of active tuberculosis. Front Immunol. 2018;9:798.
6. Valledor AF, Hsu LC, Ogawa S, Sawka-Verhelle D, Karin M, Glass CK. Activation of liver X receptors and retinoid X receptors prevents bacterial-induced macrophage apoptosis. Proc Natl Acad Sci USA. 2004;101(51):17813–8.
7. Hamada M, Nakamura M, Tran MT, Moriguchi T, Hong C, Ohsumi T, et al. MafB promotes atherosclerosis by inhibiting foam-cell apoptosis. Nat Commun. 2014;5:3147.
8. Miyazaki T, Hirokami Y, Matsuhashi N, Takatsuka H, Naito M. Increased susceptibility of thymocytes to apoptosis in mice lacking AIM, a novel murine macrophage-derived soluble factor belonging to the scavenger receptor cysteine-rich domain superfamily. J Exp Med. 1999;189(2):413–22.
9. Sarrias MR, Roselló S, Sánchez-Barbero F, Sierra JM, Vila J, Yélamos J, et al. A role for human Sp alpha as a pattern recognition receptor. J Biol Chem. 2005;280(42):35391–8.
10. Martinez VG, Escoda-Ferran C, Tadeu Simões I, Arai S, Orta Mascaró M, Carreras E, et al. The macrophage soluble receptor AIM/Api6/CD5L displays a broad pathogen recognition spectrum and is involved in early response to microbial aggression. Cell Mol Immunol. 2014;11(4):343–54.
11. Sanjurjo L, Amézaga N, Aran G, Naranjo-Gómez M, Arias L, Armengol C, et al. The human CD5L/AIM-CD36 axis: a novel autophagy inducer in macrophages that modulates inflammatory responses. Autophagy. 2015;11(3):487–502.
12. Wang C, Yosef N, Gaublomme J, Wu C, Lee Y, Clish CB, et al. CD5L/AIM regulates lipid biosynthesis and restrains Th17 cell pathogenicity. Cell. 2015;163(6):1413–27.
13. Sanchez-Moral L, Ràfols N, Martori C, Paul T, Téllez É, Sarrias MR. Multifaceted roles of CD5L in infectious and sterile inflammation. Int J Mol Sci. 2021;22(8):4076.
14. Gideon HP, Hughes TK, Tzouanas CN, Wadsworth MH, Tu AA, Gierahn TM, et al. Multimodal profiling of lung granulomas in macaques reveals cellular correlates of tuberculosis control. Immunity. 2022;55(5):827–846.e10.
15. Oliveira L, Silva MC, Gomes AP, Santos RF, Cardoso MS, Nóvoa A, et al. CD5L as a promising biological therapeutic for treating sepsis. Nat Commun. 2024;15(1):4119.
16. Maceiras AR, Silvério D, Gonçalves R, Cardoso MS, Saraiva M. Infection with hypervirulent *Mycobacterium tuberculosis* triggers emergency myelopoiesis but not trained immunity. Front Immunol. 2023;14:1211404.
17. Fonseca KL, Maceiras AR, Matos R, Simoes-Costa L, Sousa J, Cá B, et al. Deficiency in the glycosyltransferase Gcnt1 increases susceptibility to tuberculosis through a mechanism involving neutrophils. Mucosal Immunol. 2020;13(5):836–48.

18. Lai X, Wang J, Duan J, Gong Y, Cao J. Apoptosis inhibitor of macrophage differentiates bacteria from influenza or COVID-19 in hospitalized adults with community-acquired pneumonia. J Infect. 2022;84(4):579–613.
19. Gao X, Liu Y, Xu F, Lin S, Song Z, Duan J, et al. Assessment of apoptosis inhibitor of macrophage/CD5L as a biomarker to predict mortality in the critically ill with sepsis. Chest. 2019; 156(4):696–705.
20. Peters KE, Davis WA, Ito J, Winfield K, Stoll T, Bringans SD, et al. Identification of novel circulating biomarkers predicting rapid decline in renal function in type 2 diabetes: the Fremantle diabetes study phase II. Diabetes Care. 2017;40(11): 1548–55.
21. Bárcena C, Aran G, Perea L, Sanjurjo L, Téllez É, Oncins A, et al. CD5L is a pleiotropic player in liver fibrosis controlling damage, fibrosis and immune cell content. EBioMedicine. 2019;43:513–24.
22. Lai X, Xiang Y, Zou L, Li Y, Zhang L. Elevation of serum CD5L concentration is correlated with disease activity in patients with systemic lupus erythematosus. Int Immunopharmacol. 2018;63:311–6.
23. Moreira-Teixeira L, Tabone O, Graham CM, Singhania A, Stavropoulos E, Redford PS, et al. Mouse transcriptome reveals potential signatures of protection and pathogenesis in human tuberculosis. Nat Immunol. 2020;21(4):464–76.
24. Moreira-Teixeira L, Stimpson PJ, Stavropoulos E, Hadebe S, Chakravarty P, Ioannou M, et al. Type I IFN exacerbates disease in tuberculosis-susceptible mice by inducing neutrophil-mediated lung inflammation and NETosis. Nat Commun. 2020;11(1):5566.
25. Ordway D, Henao-Tamayo M, Harton M, Palanisamy G, Troudt J, Shanley C, et al. The hypervirulent *Mycobacterium tuberculosis* strain HN878 induces a potent TH1 response followed by rapid down-regulation. J Immunol. 2007;179(1): 522–31.
26. Weng D, Gao S, Shen H, Yao S, Huang Q, Zhang Y, et al. CD5L attenuates allergic airway inflammation by expanding CD11c. Immunology. 2022;167(3):384–97.
27. Sanjurjo L, Aran G, Téllez É, Amézaga N, Armengol C, López D, et al. CD5L promotes M2 macrophage polarization through autophagy-mediated upregulation of ID3. Front Immunol. 2018;9:480.
28. Gao X, Yan X, Zhang Q, Yin Y, Cao J. CD5L contributes to the pathogenesis of methicillin-resistant *Staphylococcus aureus*-induced pneumonia. Int Immunopharmacol. 2019; 72:40–7.
29. Cardoso MS, Santos RF, Almeida S, Sá M, Pérez-Cabezas B, Oliveira L, et al. Physical interactions with bacteria and protozoan parasites establish the scavenger receptor SSC4D as a broad-spectrum pattern recognition receptor. Front Immunol. 2021;12:760770.
30. Rajaram MV, Ni B, Dodd CE, Schlesinger LS. Macrophage immunoregulatory pathways in tuberculosis. Semin Immunol. 2014;26(6):471–85.
31. Ahmad F, Rani A, Alam A, Zarin S, Pandey S, Singh H, et al. Macrophage: a cell with many faces and functions in tuberculosis. Front Immunol. 2022;13:747799.
32. Zhang B, Ma X, Lin Z, Liu Y. CD5L is a potential hepatocellular carcinoma biomarker for clinical prognostic and immunotherapy. Pre-print from Research Square. 16 Feb 2023.
33. Gaublomme JT, Yosef N, Lee Y, Gertner RS, Yang LV, Wu C, et al. Single-cell genomics unveils critical regulators of Th17 cell pathogenicity. Cell. 2015;163(6):1400–12.
34. Hasegawa H, Mizoguchi I, Orii N, Inoue S, Katahira Y, Yoneto T, et al. IL-23p19 and CD5 antigen-like form a possible novel heterodimeric cytokine and contribute to experimental autoimmune encephalomyelitis development. Sci Rep. 2021; 11(1):5266.
35. Abdi K, Singh NJ, Spooner E, Kessler BM, Radaev S, Lantz L, et al. Free IL-12p40 monomer is a polyfunctional adaptor for generating novel IL-12-like heterodimers extracellularly. J Immunol. 2014;192(12):6028–36.
36. Trinchieri G. Interleukin-12 and its role in the generation of TH1 cells. Immunol Today. 1993;14(7):335–8.
37. Murphy CA, Langrish CL, Chen Y, Blumenschein W, McClanahan T, Kastelein RA, et al. Divergent pro- and antiinflammatory roles for IL-23 and IL-12 in joint autoimmune inflammation. J Exp Med. 2003;198(12):1951–7.
38. Fiorentino DF, Zlotnik A, Vieira P, Mosmann TR, Howard M, Moore KW, et al. IL-10 acts on the antigen-presenting cell to inhibit cytokine production by Th1 cells. J Immunol. 1991; 146(10):3444–51.

SUPPORTING INFORMATION

Additional supporting information can be found online in the Supporting Information section at the end of this article.

How to cite this article: Cardoso MS, Gonçalves R, Oliveira L, Silvério D, Téllez É, Paul T, et al. CD5L is upregulated upon infection with *Mycobacterium tuberculosis* with no effect on disease progression. Immunology. 2024;173(2): 310–20. https://doi.org/10.1111/imm.13825